Interferon Resistance of Emerging SARS-CoV-2 Variants

Kejun Guo[1], Bradley S. Barrett[1], Kaylee L. Mickens[1,2], Kim J. Hasenkrug[3]

and Mario L. Santiago[1,2]*

[1]*Division of Infectious Diseases, Department of Medicine,*

University of Colorado Anschutz Medical Campus, Aurora, CO, USA 80045

[2]*Department of Immunology and Microbiology,*

University of Colorado Anschutz Medical Campus, Aurora, CO, USA 80045

[3]*Rocky Mountain Laboratories, National Institutes of Allergy and Infectious Diseases,*

National Institutes of Health, Hamilton, MT 59840

*To whom correspondence should be addressed: mario.santiago@ucdenver.edu

The emergence of SARS-CoV-2 variants with enhanced transmissibility, pathogenesis and resistance to vaccines presents urgent challenges for curbing the COVID-19 pandemic. While Spike mutations that enhance virus infectivity may drive the emergence of these novel variants, studies documenting a critical a role for interferon responses in the early control of SARS-CoV-2 infection, combined with the presence of viral genes that limit these responses, suggest that interferons may also influence SARS-CoV-2 evolution. Here, we compared the potency of 17 different human interferons against 5 viral lineages sampled during the course of the global outbreak that included ancestral and emerging variants. Our data revealed increased interferon resistance in emerging SARS-CoV-2 variants, indicating that evasion of innate immunity is a significant driving force for SARS-CoV-2 evolution. These findings have implications for the increased lethality of emerging variants and highlight the interferon subtypes that may be most successful in the treatment of early infections.

The human genome encodes a diverse array of antiviral interferons (IFNs). These include the type I IFNs (IFN-Is) such as the 12 IFNα subtypes, IFNβ and IFNω that signal through ubiquitous IFNAR receptor, and the type III IFNs (IFN-IIIs) such as IFNλ1, IFNλ2 and IFNλ3 that signal through the more restricted IFNλR receptor that is present in lung epithelial cells[1]. IFN diversity may be driven by an evolutionary arms-race to enable the host to counteract diverse viral pathogens[2]. For instance, the IFNα subtypes exhibit >78% amino acid sequence identity, but IFNα14, IFNα8 and IFNα6 most potently inhibited HIV-1 *in vitro* and *in vivo*[3-5], whereas IFNα5 most potently inhibited influenza H3N2 in lung explant cultures[6]. Surprisingly, while SARS-CoV-2 was sensitive to IFNα2, IFNβ, and IFNλ[7-9], and clinical trials on IFNα2 and IFNβ demonstrated

43 promising outcomes against COVID-19[10-12], a direct comparison of multiple IFN-Is and IFN-IIIs
44 against diverse SARS-CoV-2 isolates has not yet been undertaken.
45

46 ## Results

47 The current study was undertaken to determine which IFNs would best inhibit SARS-CoV-2. We
48 selected 5 isolates from prominent lineages[13] during the course of the pandemic (Fig. 1,
49 Supplementary Table 1). USA-WA1/2020 is the standard strain utilized in many *in vitro* and *in*
50 *vivo* studies of SARS-CoV-2 and belongs to lineage A[13]. It was isolated from the first COVID-19
51 patient in the US, who had a direct epidemiologic link to Wuhan, China, where the virus was first
52 detected[14]. By contrast, subsequent infection waves from Asia to Europe[15] were associated with
53 the emergence of the D614G mutation[16]. D614G+ strains in lineage B spread with devastating
54 speed, likely due to its increased transmissibility[17,18]. It accumulated additional mutations in Italy
55 as lineage B.1 which then precipitated a severe outbreak in New York City[19]. More recently,
56 lineage B.1.1.7 acquired the N501Y mutation that is associated with enhanced transmissibility in
57 the United Kingdom[13]. Lineage B.1.351 was first reported in South Africa and acquired an
58 additional E484K mutation that is associated with resistance to neutralizing antibodies[20,21]. Both
59 B.1.1.7 and B.1.351 have now been reported in multiple countries and there is increasing concern
60 that these may become dominant[22]. Representative SARS-CoV-2 isolates from the B, B.1, B.1.1.7
61 and B.1.351 lineages were obtained from BEI Resources (Supplementary Table 1) and amplified
62 once in an alveolar type II epithelial cell line, A549, that we stably transduced with the receptor
63 ACE2 (A549-ACE2) (Supplementary Fig. 1a).
64

A549-ACE2 cells were pre-incubated with 17 recombinant IFNs (PBL Assay Science) overnight in parallel and in triplicate, then infected with a non-saturating virus dose for 2 h (Supplementary Fig. 1b). We normalized the IFNs based on molar concentrations similar to our previous work with HIV-1[3,23]. For rapid and robust evaluation of antiviral activities against live SARS-CoV-2 isolates, we utilized a quantitative PCR approach (Fig. 2a). An initial dose-titration study showed that a 2 pM concentration maximally distinguished the antiviral activities of IFNβ and IFNλ1 (Supplementary Fig. 1c), and was therefore used to screen the antiviral IFNs. In the absence of IFN, all 5 isolates reached titers of ~10^4-10^6 copies per 5 µl input of RNA extract (Fig. 2). Using absolute copy numbers (Fig. 2) and values normalized to mock as 100% (Supplementary Fig. 2), the 17 IFNs showed a range of antiviral activities against SARS-CoV-2. The 3 IFNλ subtypes exhibited none to very weak (<2-fold) antiviral activities compared to most IFN-Is (Fig. 2 and Supplementary Fig. 2, blue bars). This was despite the fact that the assay showed a robust dynamic range, with some IFNs inhibiting USA-WA1/2020 >2500-fold to below detectable levels (Fig. 2a). IFN potencies against the 5 isolates correlated with each other (Supplementary Fig. 3), and a similar rank-order of IFN antiviral potency was observed for D614G+ isolates (Fig. 2b, Supplementary Fig. 2). Overall, IFNα8, IFNβ and IFNω were the most potent, followed by IFNα5, IFNα17 and IFNα14 (Fig. 2c).

We reported that HIV-1 inhibition by the IFNα subtypes correlated with IFNAR signaling capacity and binding affinity to the IFNAR2 subunit[3,23]. IFNAR signaling capacity, as measured in an IFN-sensitive reporter cell line (iLite cells; Euro Diagnostics), correlated with the antiviral potencies of the IFNα subtypes against SARS-CoV-2 lineages A and B, but not B.1, B.1.351 or B.1.1.7 strains (Fig. 3a). Interestingly, IFNα subtype inhibition of SARS-CoV-2 did not correlate with IFNAR2

binding affinity (Fig. 3b)[24], as measured by surface plasmon resonance by the Schreiber group[24]. Furthermore, correlations between SARS-CoV-2 and HIV-1 inhibition[3] were weak at best (Fig. 3c). These findings suggested that IFN-mediated control of SARS-CoV-2 isolates may be qualitatively distinct from that of HIV-1.

We generated a heat-map to visualize the antiviral potency of diverse IFNs against the 5 isolates and observed marked differences in IFN sensitivities (Fig. 4a). Pairwise analysis of antiviral potencies between isolates collected early (January 2020) and later (March-December 2020) during the pandemic were performed against the 14 IFN-Is (IFN-IIIs were not included due to low inhibition, Fig. 2). The overall IFN-I sensitivity of USA-WA1/2020 and Germany/BavPat1/2020 isolates were not significantly different from each other (Fig. 4b). By contrast, relative to Germany/BavPat1/2020, we observed 17 to 122-fold IFN-I resistance of the emerging SARS-CoV-2 variants (Fig. 4c), with the B.1.1.7 strain exhibiting the highest IFN-I resistance. The level of interferon resistance was more striking when compared to USA-WA1/2020, where emerging SARS-CoV-2 variants exhibited 25 to 322-fold higher IFN-I resistance (Supplementary Fig. 4a).

The experiments above allowed the simultaneous analysis of 17 IFNs against multiple SARS-CoV-2 isolates, but do not provide information on how different IFN-I doses affect virus replication. It also remains unclear if the emerging variants were resistant to IFN-IIIs. We therefore titrated a potent (IFNβ; 0.002 to 200 pM) and a weak (IFNλ1; 0.02 to 2000 pM) interferon against the lineage B, B.1, B.1.1.7 and B.1.351 isolates (Fig. 4d and Supplementary Fig. 4b). We included an additional B.1.1.7 strain, hCov-19/England/204820464/2020 (Supplementary Table 1). The 50% inhibitory concentrations (IC_{50}) of the B.1.1.7 variants were 4.3 to 8.3-fold higher for IFNβ

and 3.0 to 3.5 higher for IFNλ1 than the lineage B isolate (Fig. 4d), whereas the B.1 isolate exhibited 2.6 and 5.5-fold higher IC_{50} for IFNλ1 and IFNβ, respectively (Supplementary Fig. 4b). Interestingly, maximum inhibition was not achieved with either IFNβ or IFNλ1 against the B.1.1.7 variant, plateauing at 15 to 20-fold higher levels than the ancestral lineage B isolate (Fig. 4d). In a separate experiment, the B.1.351 variant was also more resistant to IFNβ (>500-fold) and IFNλ1 (26-fold) compared to the lineage B isolate (Fig. 4d). These data confirm that the B.1, B.1.1.7 and B.1.351 isolates have evolved to resist the IFN-I and IFN-III response.

Discussion

Numerous studies done by many laboratories highlighted the importance of IFNs in SARS-CoV-2 control. Here, we demonstrate the continued evolution of SARS-CoV-2 to escape IFN responses and identify the IFNs with the highest antiviral potencies. IFNλ initially showed promise as an antiviral that can reduce inflammation[25], but was recently associated with virus-induced lung pathology[26]. Our data suggests that higher doses of IFNλ may be needed to achieve a similar antiviral effect *in vivo* as the IFN-Is. Nebulized IFNβ showed potential as a therapeutic against COVID-19[11], and our data confirm IFNβ as a highly potent antiviral against SARS-CoV-2. However, IFNβ was also linked to pathogenic outcomes in chronic mucosal HIV-1[23], murine LCMV[27] and if administered late in mice, SARS-CoV-1 and MERS-CoV[28,29] infection. By contrast, IFNα8 altered 3-fold less genes in primary mucosal lymphocytes than IFNβ[23], but showed similar anti-SARS-CoV-2 potency as IFNβ. IFNα8 also exhibited high antiviral activity against HIV-1[3], raising its potential for treatment against both pandemic viruses. Notably, IFNα8 appeared to be an outlier, as the antiviral potencies of the IFNα subtypes against SARS-CoV-2 and HIV-1 did not strongly correlate. IFNα6 potently restricted HIV-1[3,4] but was one of the weakest IFNα

subtypes against SARS-CoV-2. Conversely, IFNα5 strongly inhibited SARS-CoV-2, but weakly inhibited HIV-1[3]. Our data strengthens the theory that diverse IFNs may have evolved to restrict distinct virus families[2,23]. The mechanisms underlying these qualitative differences remain unclear. While IFNAR signaling contributes to antiviral potency[3,4,24], diverse IFNs may have distinct abilities to mobilize antiviral effectors in specific cell types. Comparing the interferomes induced by distinct IFNs in lung epithelial cells may help unravel antiviral mechanisms that is responsible for the differential effects.

Our data unmasked a concerning trend for emerging SARS-CoV-2 variants to resist the antiviral IFN response. Prior to this work, the emergence and fixation of variants was linked to enhanced viral infectivity due to mutations in the Spike protein[13,16-18]. However, previous studies on HIV-1 infection suggested that IFNs can also shape the evolution of pandemic viruses[30,31]. In fact, SARS-CoV-2 infected individuals with either genetic defects in IFN signaling[32] or IFN-reactive autoantibodies[33] had increased risk of developing severe COVID-19. As IFNs are critical in controlling early virus infection levels, IFN-resistant SARS-CoV-2 variants may produce higher viral loads that could in turn promote transmission and/or exacerbate pathogenesis. Consistent with this hypothesis, alarming preliminary reports linked B.1.1.7 with increased viral loads[34] and risk of death[35-37]. In addition to Spike, emerging variants exhibited mutations in nucleocapsid, membrane and nonstructural proteins NSP3, NSP6 and NSP12 (Supplementary Table 1). These viral proteins were shown to antagonize IFN signaling in cells[38-40]. It will be important to identify the virus mutations driving IFN-I resistance in emerging variants, the underlying molecular mechanisms, and its consequences for COVID-19 pathogenesis.

Overall, the current study suggested a role for the innate immune response in driving the evolution of SARS-CoV-2 that could have practical implications for interferon-based therapies. Our findings reinforce the importance of continued full-genome surveillance of SARS-CoV-2, and assessments of emerging variants not only for resistance to vaccine-elicited neutralizing antibodies, but also for evasion of the host interferon response.

Materials and Methods

Cell lines. A549 cells were obtained from the American Type Culture Collection (ATCC) and cultured in complete media containing F-12 Ham's media (Corning), 10% fetal bovine serum (Atlanta Biologicals), 1% penicillin/streptomycin/glutamine (Corning) and maintained at 37°C 5% CO_2. A549 cells were transduced with codon-optimized human ACE2 (Genscript) cloned into pBABE-puro[41] (Addgene). To generate the A549-ACE2 stable cell line, 10^7 HEK293T (ATCC) cells in T-175 flasks were transiently co-transfected with 60 µg mixture of pBABE-puro-ACE2, pUMVC, and pCMV-VSV-G at a 10:9:1 ratio using a calcium phosphate method[42]. Forty-eight hours post transfection, the supernatant was collected, centrifuged at 1000×*g* for 5 min and passed through a 0.45 µm syringe filter to remove cell debris. The filtered virus was mixed with fresh media (30% vol/vol) that included polybrene (Sigma) at a 6 µg/ml final concentration. The virus mixture was added into 6-well plates with 5×10^5 A549 cells/well and media was changed once more after 12 h. Transduced cells were selected in 0.5 µg/ml puromycin for 72 h, and ACE2 expression was confirmed by flow cytometry, western blot and susceptibility to HIV-1ΔEnv/SARS-CoV-2 Spike pseudovirions.

Virus isolates. All experiments with live SARS-CoV-2 were performed in a Biosafety Level-3 (BSL3) facility with powered air-purifying respirators at the University of Colorado Anschutz Medical Campus. SARS-CoV-2 stocks from BEI Resources (Supplementary Table 1) had comparable titers $>10^6$ $TCID_{50}$/ml (Supplementary Fig. 1a) except for the B.1.1.7 strains (CA_CDC_5574/2020 and England/204820464/2020). The contents of the entire vial (~0.5 ml) were inoculated into 3 T-75 flasks containing 3×10^6 A549-ACE2 cells, except for B.1.1.7 which was inoculated into 1 T-75 flask. After culturing for 72 h, the supernatants were collected and spun at 2700×*g* for 5 min to remove cell debris, and frozen at -80°C. The A549-amplified stocks were titered according to the proposed assay format (Supplementary Fig. 1b, Fig. 2a). Briefly, 2.5×10^4 A549-ACE2 cells were plated per well in a 48-well plate overnight. The next day, the cells were infected with 300, 30, 3, 0.3, 0.03 and 0.003 µl (serial 10-fold dilution) of amplified virus stock in 300 µl final volume of media for 2 h. The virus was washed twice with PBS, and 500 µl of complete media with the corresponding IFN concentrations were added. After 24 h, supernatants were collected, and cell debris was removed by centrifugation at 3200×*g* for 5 min.

SARS-CoV-2 quantitative PCR. For rapid and robust assessments of viral replication, we utilized a real-time quantitative PCR (qPCR) approach. This assay would require less handling of infectious, potentially high-titer SARS-CoV-2 in the BSL3 compared to a VeroE6 plaque assay, as the supernatants can be directly placed in lysis buffer containing guanidinium thiocyanate that would inactivate the virus by at least 4-5 $\log_{10}$[43]. To measure SARS-CoV-2 levels, total RNA was extracted from 100 µl of culture supernatant using the E.Z.N.A Total RNA Kit I (Omega Bio-Tek) and eluted in 50 µl of RNAse-free water. 5 µl of this extract was used for qPCR. Official CDC

SARS-CoV-2 N1 primers and TaqMan probe set were used[44] with the Luna Universal Probe One-Step RT-qPCR Kit (New England Biolabs):

Forward primer: `GACCCCAAAATCAGCGAAAT`

Reverse primer: `TCTGGTTACTGCCAGTTGAATCTG`

TaqMan probe: `FAM-ACCCCGCATTACGTTTGGTGGACC-TAMRA`

The sequence of the primers and probes were conserved against the 5 SARS-CoV-2 variants that were investigated. The real-time qPCR reaction was run on a Bio-Rad CFX96 real-time thermocycler under the following conditions: 55°C 10 mins for reverse transcription, then 95°C 1 min followed by 40 cycles of 95°C 10s and 60°C 30s. The absolute quantification of the N1 copy number was interpolated using a standard curve with 10^7-10^1 serial 10-fold dilution of a control plasmid (nCoV-CDC-Control Plasmid, Eurofins).

Antiviral inhibition assay. We used a non-saturating dose of the amplified virus stock for the IFN inhibition assays. These titers were expected to yield ~10^5 copies per 5 µl input RNA extract (Supplementary Fig. 1b). Recombinant IFNs were obtained from PBL Assay Science. In addition to the IFN-Is (12 IFNα subtypes, IFNβ and IFNω), we also evaluated 3 IFNλ subtypes (IFNλ1, IFNλ2, IFNλ3). To normalize the IFNs, we used molar concentrations[23] instead of international units (IU), as IU values were derived from inhibition of encelphalomyocarditis virus, which may not be relevant to SARS-CoV-2. To find a suitable dose to screen 17 IFNs in parallel, we performed a dose-titration experiment of the USA-WA1/2020 strain with IFNβ and IFNλ1. A dose of 2 pM allowed for maximum discrimination of the antiviral potency IFNβ versus IFNλ1 (Supplementary Fig. 1c). Serial 10-fold dilutions of IFNβ and IFNλ1 were also used in follow-up experiments. Thus, in 48-well plates, we pre-incubated 2.5×10^4 A549-ACE2 cells with the IFNs

for 18 h, then infected with the A549-amplified virus stock for 2 h. After two washes with PBS, 500 µl complete media containing the corresponding IFNs were added. The cultures were incubated for another 24 h, after which, supernatants were harvested for RNA extraction and qPCR analysis.

Statistical analyses. Data were analyzed using GraphPad Prism 8. Differences between the IFNs were tested using a nonparametric two-way analysis of variance (ANOVA) followed by a multiple comparison using the Friedman test. Pearson correlation coefficients (R^2) values were computed for linear regression analyses. Paired analysis of two isolates against multiple IFNs were performed using a nonparametric, two-tailed Wilcoxon matched-pairs rank test. Differences with $p<0.05$ were considered significant. Nonlinear regression curves were fit using a two-phase exponential decay equation on log-transformed data.

Acknowledgments

We thank Cara Wilson, Ulf Dittmer and Kathrin Gibbert for scientific advice; Mercedes Rincon and Elan Eisenmesser for assistance with construction and characterization of the A549-ACE2 cells; Eric Poeschla, James Morrison, Zach Wilson, Jill Garvey, Stephanie Torres-Nemeti and Marcia Finucane for Biosafety Level-3 infrastructure support; and Roman Wölfel, Rosina Ehmann, Adolfo García-Sastre, Alex Sigal, Tulio de Oliveira, Bassam Hallis, the CDC and BEI Resources (NIAID) for the SARS-CoV-2 isolates. This work was supported by the Department of Medicine at the University of Colorado (MLS), NIH R01 AI134220 (MLS), and the Intramural Research Program at the NIH, NIAID (KJH).

Figures

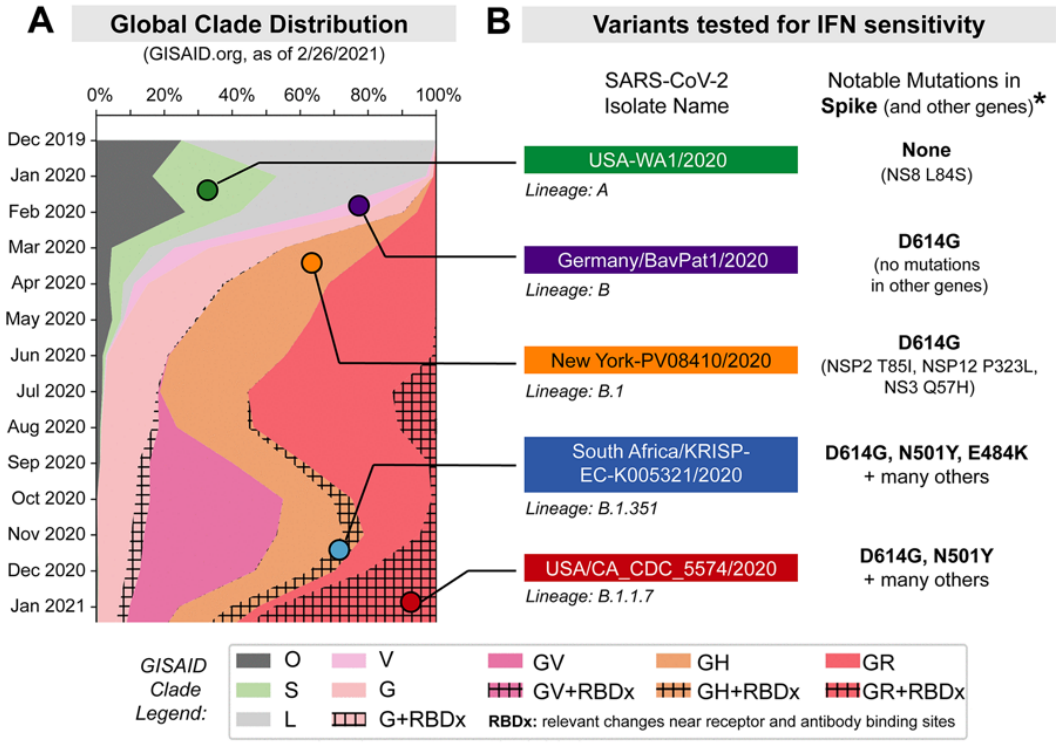

Figure 1 | Selection of SARS-CoV-2 strains for IFN sensitivity studies. (**a**) Global distribution of SARS-CoV-2 clades. GISAID.org plotted the proportion of deposited sequences in designated clades against collection dates. The five isolates chosen are noted by colored dots. (**b**) SARS-CoV-2 strains selected for this study included representatives of lineages A, B, B.1, B.1.351 and B.1.1.7 (Supplementary Table 1). Lineage B isolates encode the D614G mutation associated with increased transmissibility. *Amino acid mutations were relative to the reference hCOV-19/Wuhan/WIV04/2019 sequence.

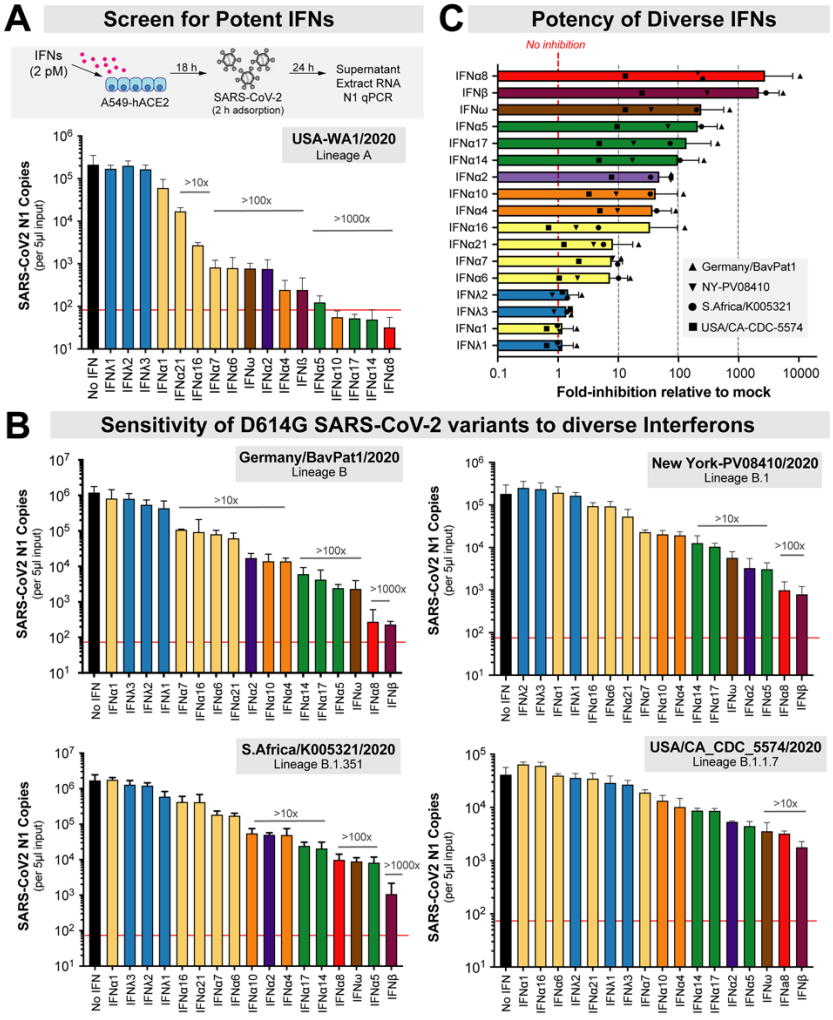

Figure 2 | Sensitivity of SARS-CoV-2 strains to IFN-I and IFN-III interferons. (**a**) Antiviral assay using recombinant IFNs (2 pM) in A549-ACE2 cells. The red line corresponds to the qPCR detection limit (<90 copies/reaction). (**b**) Viral copy numbers in D614G+ isolates, showing a similar rank-order of IFNs from least to most potent. (**c**) The average fold-inhibition relative to mock for lineage B, B.1, B.1.351 and B.1.1.7 isolates are shown. The most potent IFNs are shown top to bottom. For all panels, bars and error bars correspond to means and standard deviations.

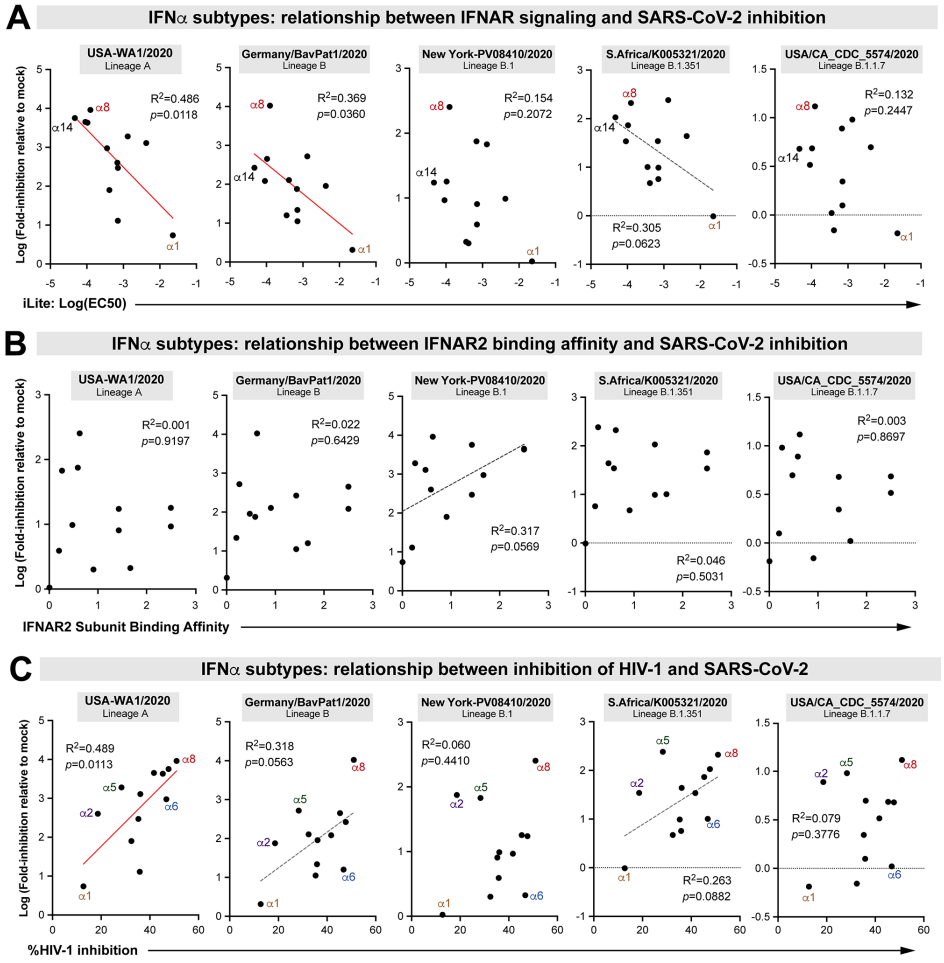

Figure 3 | Correlation between SARS-CoV-2 inhibition and biological properties of IFNα subtypes. Log-transformed IFN-inhibition values relative to mock for the 5 different SARS-CoV-2 strains were compared to previously published values on (**a**) 50% effective concentrations in the iLite assay, a reporter cell line encoding the IFN sensitive response element of *ISG15* linked to firefly luciferase[23]; (**b**) IFNAR2 subunit binding affinity, as measured by surface plasmon resonance by the Schreiber group[24]; and (**c**) HIV-1 inhibition values, based on % inhibition of HIV-1 p24+ gut lymphocytes relative to mock as measured by flow cytometry[3]. Each dot corresponds to an IFNα subtype. Linear regression was performed using GraphPad Prism 8. Significant correlations ($p<0.05$) were highlighted with a red best-fit line; those that were trending ($p<0.1$) had a gray, dotted best-fit line.

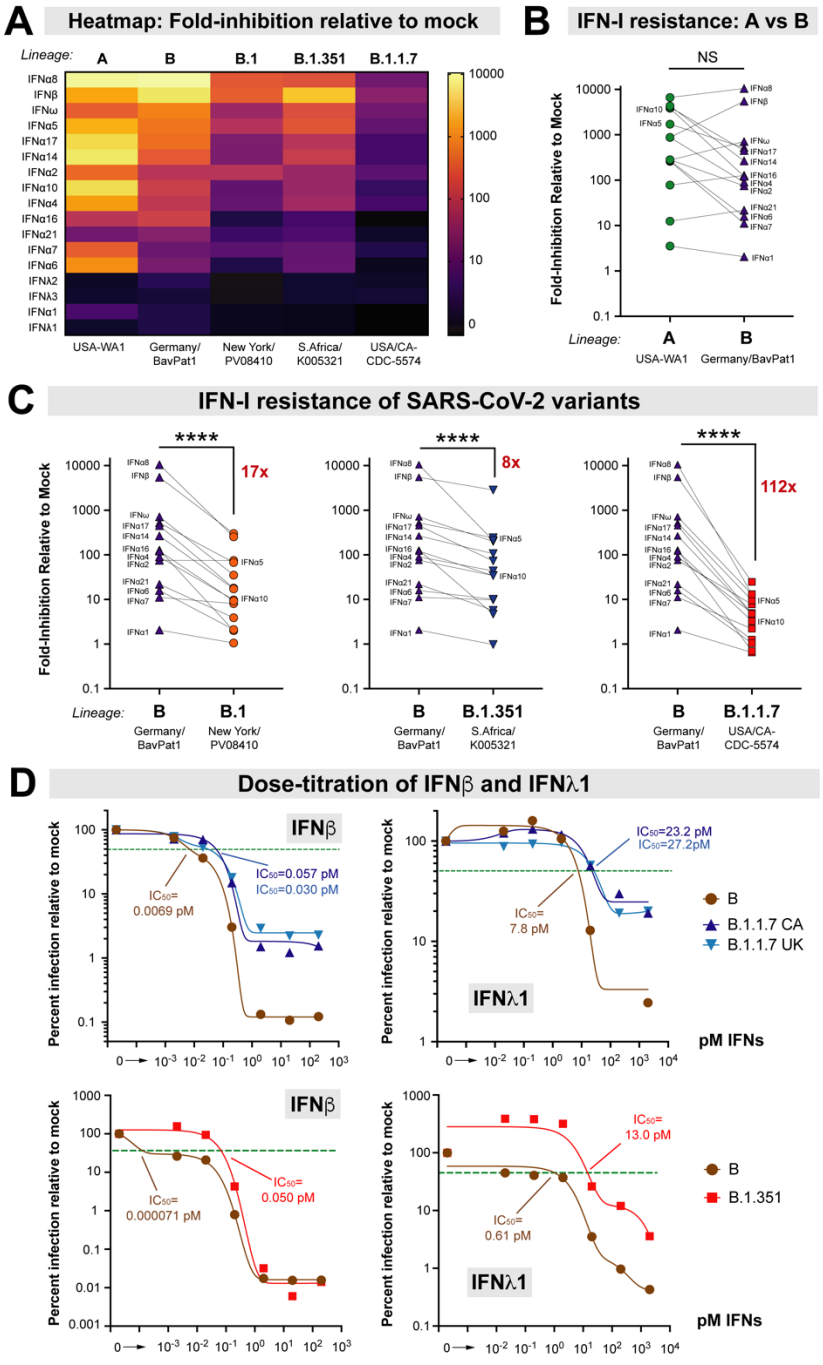

Figure 4 | Increased interferon resistance of emerging SARS-CoV-2 variants. (**a**) Heatmap of fold-inhibition of representative strains from the lineages noted. Colors were graded on a log-scale from highest inhibition (yellow) to no inhibition (black). Comparison of IFN-I sensitivities between (**b**) lineage A and B isolates; and (**c**) lineage B versus B.1, B.1.351 and B.1.1.7. The mean fold-inhibition values relative to mock were compared in a pairwise fashion for the 14 IFN-Is. In

(**c**), the average fold-inhibition values were noted. Differences were evaluated using a nonparametric, two-tailed Wilcoxon matched-pairs signed rank test. NS, not significant; ****, $p<0.0001$. (**d**) Dose-titration of IFNβ and IFNλ1 against lineage B (Germany/BavPat1/2020) versus B.1.1.7 and B.1.351 isolates. In addition to USA/CA_CDC_5574/2020, we also evaluated a second B.1.1.7 isolate from the United Kingdom (UK), England/204820464/2020. A549-ACE2 cells were pre-treated with serial 10-fold dilutions of IFNs for 18 h in triplicate and then infected with SARS-CoV-2. Supernatants were collected after 24 h, SARS-CoV-2 N1 copy numbers were determined by qPCR, and then normalized against mock as 100%. Non-linear best-fit regression curves of mean normalized infection levels were used to interpolate 50% inhibitory concentrations (green dotted lines).

References

1 Pestka, S., Krause, C. D. & Walter, M. R. Interferons, interferon-like cytokines, and their receptors. *Immunol Rev* **202**, 8-32, doi:10.1111/j.0105-2896.2004.00204.x (2004).

2 Gibbert, K., Schlaak, J. F., Yang, D. & Dittmer, U. IFN-alpha subtypes: distinct biological activities in anti-viral therapy. *Br J Pharmacol* **168**, 1048-1058, doi:10.1111/bph.12010 (2013).

3 Harper, M. S. *et al.* Interferon-alpha Subtypes in an Ex Vivo Model of Acute HIV-1 Infection: Expression, Potency and Effector Mechanisms. *PLoS Pathog* **11**, e1005254, doi:10.1371/journal.ppat.1005254 (2015).

4 Schlaepfer, E. *et al.* Dose-Dependent Differences in HIV Inhibition by Different Interferon Alpha Subtypes While Having Overall Similar Biologic Effects. *mSphere* **4**, doi:10.1128/mSphere.00637-18 (2019).

5 Lavender, K. J. *et al.* Interferon Alpha Subtype-Specific Suppression of HIV-1 Infection In Vivo. *J Virol* **90**, 6001-6013, doi:10.1128/JVI.00451-16 (2016).

6 Matos, A. D. R. *et al.* Antiviral potential of human IFN-alpha subtypes against influenza A H3N2 infection in human lung explants reveals subtype-specific activities. *Emerg Microbes Infect* **8**, 1763-1776, doi:10.1080/22221751.2019.1698271 (2019).

7 Vanderheiden, A. *et al.* Type I and Type III Interferons Restrict SARS-CoV-2 Infection of Human Airway Epithelial Cultures. *J Virol* **94**, doi:10.1128/JVI.00985-20 (2020).

8 Felgenhauer, U. *et al.* Inhibition of SARS-CoV-2 by type I and type III interferons. *The J Biol Chem* **295**, 13958-13964, doi:10.1074/jbc.AC120.013788 (2020).

9 Nchioua, R. *et al.* SARS-CoV-2 Is Restricted by Zinc Finger Antiviral Protein despite Preadaptation to the Low-CpG Environment in Humans. *mBio* **11**, doi:10.1128/mBio.01930-20 (2020).

10 Wang, N. *et al.* Retrospective Multicenter Cohort Study Shows Early Interferon Therapy Is Associated with Favorable Clinical Responses in COVID-19 Patients. *Cell host & microbe* **28**, 455-464 e452, doi:10.1016/j.chom.2020.07.005 (2020).

11 Monk, P. D. *et al.* Safety and efficacy of inhaled nebulised interferon beta-1a (SNG001) for treatment of SARS-CoV-2 infection: a randomised, double-blind, placebo-controlled, phase 2 trial. *Lancet Respir Med*, doi:10.1016/S2213-2600(20)30511-7 (2020).

12 Shalhoub, S. Interferon beta-1b for COVID-19. *Lancet* **395**, 1670-1671, doi:10.1016/S0140-6736(20)31101-6 (2020).

13 Rambaut, A. *et al.* A dynamic nomenclature proposal for SARS-CoV-2 lineages to assist genomic epidemiology. *Nat Microbiol* **5**, 1403-1407, doi:10.1038/s41564-020-0770-5 (2020).

14 Zhou, P. *et al.* A pneumonia outbreak associated with a new coronavirus of probable bat origin. *Nature* **579**, 270-273, doi:10.1038/s41586-020-2012-7 (2020).

15 Worobey, M. *et al.* The emergence of SARS-CoV-2 in Europe and North America. *Science* **370**, 564-570, doi:10.1126/science.abc8169 (2020).

16 Korber, B. *et al.* Tracking Changes in SARS-CoV-2 Spike: Evidence that D614G Increases Infectivity of the COVID-19 Virus. *Cell* **182**, 812-827 e819, doi:10.1016/j.cell.2020.06.043 (2020).

17 Plante, J. A. *et al.* Spike mutation D614G alters SARS-CoV-2 fitness. *Nature*, doi:10.1038/s41586-020-2895-3 (2020).

18 Hou, Y. J. *et al.* SARS-CoV-2 D614G variant exhibits efficient replication ex vivo and transmission in vivo. *Science* **370**, 1464-1468, doi:10.1126/science.abe8499 (2020).

19 Gonzalez-Reiche, A. S. *et al.* Introductions and early spread of SARS-CoV-2 in the New York City area. *Science* **369**, 297-301, doi:10.1126/science.abc1917 (2020).

20 Wibmer, C. K. *et al.* SARS-CoV-2 501Y.V2 escapes neutralization by South African COVID-19 donor plasma. *Nature Med*, doi:10.1038/s41591-021-01285-x (2021).

21 Wang, P. *et al.* Antibody Resistance of SARS-CoV-2 Variants B.1.351 and B.1.1.7. *Nature*, doi:10.1038/s41586-021-03398-2 (2021).

22 Galloway, S. E. *et al.* Emergence of SARS-CoV-2 B.1.1.7 Lineage - United States, December 29, 2020-January 12, 2021. *MMWR Morb Mortal Wkly Rep* **70**, 95-99, doi:10.15585/mmwr.mm7003e2 (2021).

23 Guo, K. *et al.* Qualitative Differences Between the IFNalpha subtypes and IFNbeta Influence Chronic Mucosal HIV-1 Pathogenesis. *PLoS Pathog* **16**, e1008986, doi:10.1371/journal.ppat.1008986 (2020).

24 Lavoie, T. B. *et al.* Binding and activity of all human alpha interferon subtypes. *Cytokine* **56**, 282-289, doi:10.1016/j.cyto.2011.07.019 (2011).

25 Davidson, S. *et al.* IFNlambda is a potent anti-influenza therapeutic without the inflammatory side effects of IFNalpha treatment. *EMBO Mol Med* **8**, 1099-1112, doi:10.15252/emmm.201606413 (2016).

26 Broggi, A. *et al.* Type III interferons disrupt the lung epithelial barrier upon viral recognition. *Science* **369**, 706-712, doi:10.1126/science.abc3545 (2020).

27 Ng, C. T. *et al.* Blockade of interferon Beta, but not interferon alpha, signaling controls persistent viral infection. *Cell host & microbe* **17**, 653-661, doi:10.1016/j.chom.2015.04.005 (2015).

28 Channappanavar, R. *et al.* IFN-I response timing relative to virus replication determines MERS coronavirus infection outcomes. *J Clin Invest* **130**, 3625-3639, doi:10.1172/JCI126363 (2019).

29 Channappanavar, R. *et al.* Dysregulated Type I Interferon and Inflammatory Monocyte-Macrophage Responses Cause Lethal Pneumonia in SARS-CoV-Infected Mice. *Cell host & microbe* **19**, 181-193, doi:10.1016/j.chom.2016.01.007 (2016).

30 Iyer, S. S. *et al.* Resistance to type 1 interferons is a major determinant of HIV-1 transmission fitness. *Proc Natl Acad Sci USA* **114**, E590-E599, doi:10.1073/pnas.1620144114 (2017).

31 Parrish, N. F. *et al.* Phenotypic properties of transmitted founder HIV-1. *Proc Natl Acad Sci USA* **110**, 6626-6633, doi:10.1073/pnas.1304288110 (2013).

32 Zhang, Q. *et al.* Inborn errors of type I IFN immunity in patients with life-threatening COVID-19. *Science* **370**, doi:10.1126/science.abd4570 (2020).

33 Bastard, P. *et al.* Autoantibodies against type I IFNs in patients with life-threatening COVID-19. *Science* **370**, doi:10.1126/science.abd4585 (2020).

34 Kidd, M. *et al.* S-variant SARS-CoV-2 lineage B1.1.7 is associated with significantly higher viral loads in samples tested by ThermoFisher TaqPath RT-qPCR. *J Inf Dis*, doi:10.1093/infdis/jiab082 (2021).

35 Horby, P. *et al.* NERVTAG note on B.1.1.7 severity. (2021).

36 Davies, N. G. *et al.* Increased hazard of death in community-tested cases of SARS-CoV-2 Variant of Concern 202012/01. *medRxiv*, doi:10.1101/2021.02.01.21250959 (2021).

37 Challen, R. *et al.* Risk of mortality in patients infected with SARS-CoV-2 variant of concern 202012/1: matched cohort study. *BMJ* **372**, n579, doi:10.1136/bmj.n579 (2021).

38 Lei, X. *et al.* Activation and evasion of type I interferon responses by SARS-CoV-2. *Nat Commun* **11**, 3810, doi:10.1038/s41467-020-17665-9 (2020).

39 Xia, H. *et al.* Evasion of Type I Interferon by SARS-CoV-2. *Cell reports* **33**, 108234, doi:10.1016/j.celrep.2020.108234 (2020).

40 Mu, J. *et al.* SARS-CoV-2 N protein antagonizes type I interferon signaling by suppressing phosphorylation and nuclear translocation of STAT1 and STAT2. *Cell Discov* **6**, 65, doi:10.1038/s41421-020-00208-3 (2020).

41 Morgenstern, J. P. & Land, H. Advanced mammalian gene transfer: high titre retroviral vectors with multiple drug selection markers and a complementary helper-free packaging cell line. *Nucleic acids research* **18**, 3587-3596, doi:10.1093/nar/18.12.3587 (1990).

42 Dillon, S. M., Guo, K., Castleman, M. J., Santiago, M. L. & Wilson, C. C. Quantifying HIV-1-Mediated Gut CD4+ T Cell Death in the Lamina Propria Aggregate Culture (LPAC) Model *Bio-Protocol* **10**, doi:10.21769/BioProtoc.3486 (2020).

43 Pastorino, B. *et al.* Evaluation of Chemical Protocols for Inactivating SARS-CoV-2 Infectious Samples. *Viruses* **12**, doi:10.3390/v12060624 (2020).

44 CDC. Research Use Only 2019-Novel Coronavirus (2019-nCoV) Real-time RT-PCR Primers and Probes. https://www.cdc.gov/coronavirus/2019-ncov/lab/rt-pcr-panel-primer-probes.html. (2020).